HHS Public Access

Author manuscript

Min Metall Explor. Author manuscript; available in PMC 2023 May 11.

Published in final edited form as:

Min Metall Explor. 2022 April 14; 39: . doi:10.1007/s42461-022-00596-y.

Assessment of Floor Heave Associated with Bumps in a Longwall Mine Using the Discrete Element Method

Bo Hyun Kim[1], **Mark K. Larson**[1]

[1]Mine Safety Branch, Spokane Mining Research Division, CDC/NIOSH, 315 E Montgomery Avenue, Spokane, WA 99207, USA

Abstract

This study was developed as part of an effort by the National Institute for Occupational Safety and Health (NIOSH) to better understand rock-mass behavior in longwall coal mines in highly stressed, bump-prone ground. The floor-heave and no-floor-heave phenomena at a western US coal mine could not be properly simulated in numerical models using conventional shear-dominant failure criteria (i.e., Mohr–Coulomb or Hoek–Brown failure criterion). The previous numerical study demonstrated these phenomena using a user-defined model of the s-shaped brittle failure criterion in conjunction with a spalling process in the FLAC3D numerical modeling software. The results of the FLAC3D modeling agreed with the observations of the relative amounts of heave from each gate-road system. However, the FLAC3D model adopted many assumptions and simplifications that were not very realistic from a physical or mechanical perspective. To overcome the limitations of the FLAC3D model, 3DEC modeling in conjunction with the discrete fracture network (DFN) technique was performed to better understand the true behavior of floor heave associated with underground mining in an anisotropic stress field. The effect of stress rotation in the mining-induced stress field was considered by using a different geometry of rock fractures in the coal seam. The heterogeneity of the engineering properties (i.e., cohesion and tensile strength) were also considered by using Monte Carlo simulations. Consequently, the 3DEC models using the DFN technique resulted in predictions of floor heave that agreed with observations of the relative amounts of heave from each gate-road system, but the cause of heave was mainly related to the degree of anisotropy instead of the size of the pillar.

Keywords

Coal mine; Floor heave; 3DEC; Discrete fracture network (DFN)

1 Introduction

Floor failure in coal mines often inhibits longwall mining operations, as large displacement of floor strata, known as floor heave, interferes with travel, access, ventilation, and equipment operation. This study was developed as part of an effort by the National Institute

✉Bo Hyun Kim, BKim2@cdc.gov.

Conflict of Interest The authors declare no competing interests.

for Occupational Safety and Health (NIOSH) to better understand rock-mass behavior in longwall coal mines in highly stressed, bump-prone ground.

NIOSH researchers observed floor heave at a western US coal mine where pillar width in a three-entry gate-road system was 52 m, whereas no perceptible floor heave occurred where the pillar width in the gate-roads was 22 m (Lawson, personal communication). The floor heave most often occurred soon after development, and additional stress resulting from panel mining only increased the amount of floor heave. In addition, regular face and butt cleat systems were observed in the seam throughout the gate roads with smaller pillars, but they were variable in orientation in the seam in the gate roads with larger pillars, particularly in areas within 200 m of intersecting faults. This area of irregular cleat orientation is of particular interest because a bump later occurred with damage that included much of this area with variable cleats.

Mine engineers at two nearby mines reported the same correlation of floor heave with larger pillars, and such heave was not avoided by designing with empirical tools. The authors have personal knowledge of floor heave associated with large pillars at another mine in a different western coalfield. Mining-induced seismic events are prevalent to varying degrees at these mines. Floor heaves and bumps are often associated with one another, regardless of the bumping mechanism.

Kim and Larson [1] attempted to determine through simulation with numerical models the reasons for floor heave that they had observed—small energy releases that appeared to be associated with coal bumps. The premise of their study was that brittle rock failure is associated with both floor heave and some bump mechanisms, if not directly involved in their cause. Their models demonstrated the relative amounts of observed floor-heave/no-floor-heave phenomenon associated with pillar width changes using a user-defined model of the s-shaped brittle failure criterion in conjunction with a spalling process in FLAC3D.

However, the continuum FLAC3D model had inherent assumptions and simplifications that were not very realistic from a physical or mechanical perspective. For example, the anisotropic behavior resulting from various orientations of perpendicular cleat sets could not be explicitly simulated. To improve on the physical and mechanical realism, 3DEC [2] modeling in conjunction with the discrete fracture network (DFN) technique was performed to better approximate the contribution of cleat sets in causing floor heave associated with underground mining in an anisotropic stress field. The effect of stress rotation in a mining-induced stress field was considered by rotating the excavation and DFN with respect to the loading directions. The heterogeneity of the engineering properties (i.e., cohesion and tensile strength) was also considered by using Monte Carlo simulations.

Thus, there are two main goals of this study: first, to construct different levels of anisotropy and different cleat systems with DFNs in 3DEC, and second, to test these models to see if they can replicate the floor-heave and no-floor-heave phenomena observed and explain the influence of anisotropy and cleat development on the failure mechanisms in gate-road systems of different pillar width. In this study, the DFN is used to explicitly create the different levels of anisotropy and development of cleat sets in the coal seam of each gate-

road system. A contrasting statistical parameter is used for the realization of the DFNs. As a result, the poorly cleated coal seam with oblique angles from horizontal—where horizontal is the plane that is parallel to the simulated coal seam—is generated in the wide pillar system, and the well-cleated coal seam with subparallel angles from horizontal is generated in the narrow pillar system, respectively, as per observations. Ultimately, 3DEC analyses in conjunction with the DFNs are shown to replicate the floor-heave and no-floor-heave phenomena previously simulated using FLAC3D models (Kim and Larson [1]) and explain the influence of anisotropy and cleat development on the failure mechanism in each gate-road system.

The next section discusses cleats in coal seams and their impact on the mechanical behavior of coal. Then, the following section describes the approach used for the laboratory testing, including sample preparation and loading conditions used. Finally, the approaches for examining strength as a function of orientation between cleat and loading direction are explained, and these results are compared to analytical and numerical analysis results. Spatial characteristics of coal cleats fractures occur in nearly all coal beds and can exert a fundamental control on coal stability, minability, and fluid flow. As illustrated in Fig. 1, cleats are fractures that usually occur in two sets that are, in most instances, mutually perpendicular and also perpendicular to bedding [3].

Generally, cleats occur with spacing ranging from 1 to 6 cm. Several researchers have reported that spatial characteristics of cleats and their angle with respect to the greatest compressive principal stress direction control a coal's strength and impact the relative brittleness of the coal. For example, Agapito and Goodrich [4] reported that Western US dynamic failure events are associated with coals that are poorly cleated, indicating wider-than-usual spacing between cleat apertures. Conditions associated with the double fatality caused by a coal burst at the Austar Mine in Australia in 2014 were described by Hebblewhite and Galvin [5] as having localized variability in cleat distribution. They also described that the resultant anisotropy was influenced by the angle between the direction of mine development and the direction of the major sub-horizontal principal stress. More recently, Kim and Larson [6] and Kim et al. [7] found that cleats play a significant role in the anisotropy of strength and the degree of brittleness. Specifically, their numerical results showed that the strength was weakest, and the Hoek–Brown constant, m_i, was the greatest (or most brittle when the cleat was oriented at 30° from the axial loading direction. To be clear, the included angle between the principal stresses (as illustrated by the arrows in Fig. 1) and the orientation of the cleats governs a coal's variation in strength and behavior.

2 Methods using 3DEC and DFN Simulations for Assessment of Floor Heaves

2.1 Preparation of a 3DEC Model

A model with dimensions of 480(W) × 370(H) × 10(L) m was constructed, as illustrated in Fig. 2. Based on the field observation by Lawson (personal communication), the immediate floor in the wide pillar and in the narrow pillar was considered more anisotropic and less anisotropic material, respectively.

It was also considered that the heights of each layer of rock mass in the model are 182 m for the top, 4 m for the seam and the floor, and 178 m for the bottom layer, respectively. The depth of the top boundary of the model from the surface was set at 474.4 m below the surface (top-of-seam 656.4 m below surface). A surcharge of vertical stress was applied on the top boundary of the model to account for the weight of overburden not explicitly represented in the model. The horizontal stresses were greater than the vertical stress. It was presumed that the major principal stress (σ_H) had a magnitude (MPa) of 3.5 × overburden stress in the *y*-direction of the model. The intermediate principal stress (σ_h) had a magnitude (MPa) of 2.5 × overburden stress in the *x*-direction of the model. The minor principal stress (σ_v) had a magnitude (MPa) of the unit weight × depth [1].

For the boundary conditions, both sides of the model were fixed in the *x*-direction, and both the front and back of the model were fixed in the *y*-direction. The bottom of the model was fixed in the *z*-direction. The geometries of the gate-roads and pillars were simplified so that the gate-road entries were 6-m wide and 4-m high, leaving pillars that were 22- and 52-m wide. The equivalent zone size of the individual mesh elements in the model was set as 1 m for both the top and bottom layer of rock mass and as 0.5 m for the seam and floor, respectively.

2.2 Realization of Cleats and Bedding Planes in the Coal Seam Using DFNs

Lawson (personal communication) observed and confirmed that the orientation of cleating in the region of the wide pillar system showed a zone of localized deviation from the norm with respect to both spacing and orientation. While faulting also is noted in the area, the distribution of cleat orientation near the fault has not been quantitatively measured but has been visually estimated. This zone of cleats with a variable orientation by the fault is extended for a distance of several pillars—far beyond the spatial extent of the mapped fault plane. Similar observations were made by Robeck [8], who noted changes in cleat characteristics for a distance exceeding 30 m from visible fault planes.

The changes noted by the field observations (Lawson, personal communication, 2012) correlated with an associated zone of anomalous deterioration observed over a period of time preceding a large-scale seismic event. Although not observable, it is assumed that the cleating extended into the floor because it was composed of coal and carbonaceous mudstone (Lawson, personal communication, 2012). Similar changes in cleat characteristics were not observed in the gate road with the narrow pillar. It is, therefore, anticipated that the orientation of cleats to the loading direction driven by the major principal stress, the so-called included angle, would control the anisotropic behavior.

In this section, the built-in DFN generator in 3DEC is used to explicitly realize the spatial anisotropic characteristics of the coal seam observed from a bump-prone underground coal mine. The spatial characteristics of the discontinuities (i.e., cleats and bedding planes) as input data for the 3DEC model are estimated based on the results of the laboratory tests and field observations.

The different dip angles of the bedding planes were used to generate the DFNs that more explicitly represent two anisotropies of coal in a 480(W) × 4(H) × 10(L) m numerical

domain. Two sets of bedding planes are presented in this section, having mean dip angles of 0 and 30° from horizontal—where horizontal is the direction parallel with the seam.

The orientations of the cleats and bedding planes are plotted in a stereographic projection, as shown in Fig. 3. The Fisher distribution based on these orientations is used to generate the DFNs. The power-law distribution is chosen to determine the sizes of the cleats (0.01 to 0.1 m) and the bedding planes (100.0 to 500.0 m), respectively. The generated DFNs are illustrated in Fig. 4.

2.3 Stochastic Approach for Considering Heterogeneity of Engineering Properties by Monte Carlo Simulation

All blocks in the 3DEC model are built as deformable and elastic blocks. The DFNs are created only in the coal seam in the model. To emphasize and simulate a stress localization, the heterogeneity of the engineering properties (i.e., cohesion and tensile strength) in the 3DEC models are also considered using Monte Carlo simulations. The heterogeneous strengths can be modeled by populating the blocks and block contacts of the model with probability distributions. In the 3DEC models, the blocks are defined as elastic and zones formed with an approximate edge length of 0.1 m. The built-in Mohr C + + plug-in is used in the models [2]. To create the numerical specimens, each block contact is assigned a cohesion and a tensile strength value randomly selected from the probability distributions generated by the Monte Carlo simulation, as shown in Fig. 5. The range of the cohesion and the tensile strength is 1.35 ± 0.91 and 0.45 ± 0.30 MPa, respectively. All sub-contacts forming each contact are assigned the same tensile strength and cohesion.

Figure 5 shows the cumulative distributions of the cohesion and tensile strength, (a) and (b), and the assigned properties in the coal seam in the 3DEC model (c).

Table 1 shows the input data used for the 3DEC model. The material properties are estimated based on the results of laboratory tests [7] and field observation [9] and the literature [10–12]. Ten different 3DEC models were constructed, each having a different realization of DFN generation.

3 Results and Discussion

Kim and Larson [1] conducted the FLAC3D modeling such that where the open joints controlling rock-mass strength had a preferred orientation, ubiquitous joints (UBJ) were activated within the model with orientations that reflect the true orientation distribution. This approach, referred to as the Ubiquitous Joint Rock Mass (UJRM) model, originally was conceived by Clark [13] as a means to account for the impact of jointing on rock-mass strength more explicitly within FLAC3D by assigning a unique joint orientation to each zone. Since then, it has been extended and applied in FLAC3D to the study of cave propagation [14–16]. The introduction of ubiquitous joints in this manner implicitly introduced scale effects, anisotropy, and variability.

To be clear, in the FLAC3D model, Kim and Larson [1] treated the material properties differently in the wide pillar system than in the narrow pillar system. This assumption

was developed based on the laboratory testing results. Specifically, the material properties in the wide pillar system had lower strength and greater brittleness than the properties in the narrow pillar system. This implicit approach permitted replication of the different developing cleating systems in the coal seam that was previously observed (Lawson, personal communication).

Kim and Larson [1] also found that the dip angles of the simultaneously installed ubiquitous joints are more or less oblique within the range from 20 to 40° relative to horizontal in the wide pillar system. However, the dip angles can be found as sub-horizontal ubiquitous joints (UBJ) (< 10°) adjacent to the floor or subvertical UBJ (> 80°) adjacent to the ribs of gate-roads in the narrow pillar system. In this study, the coal properties were kept the same between the narrow and wide pillar systems. Greater anisotropy for the wide pillar system was achieved instead by the explicit introduction of DFNs, with the wide pillar system having a wider range of orientation and smaller spacing and persistence than in the narrow pillar system, where DFNs had a smaller range of orientation that was sub-horizontal or subvertical.

To create the DFNs representing the oblique included angles, based on the analysis as illustrated in Fig. 3 the Fisher constant (K) was determined as 50 and the relatively low fracture frequency, P_{10}, was from 9 to 11. The sizes of the DFNs were also chosen from 0.05 to 0.5 m. The combination of these parameters results in the poorly cleated coal seam as nonpersistent discontinuities in the wide pillar gate-roads system. Contrastively, the Fisher constant (K) was determined as 100, and the relatively high fracture frequency, P_{10}, as from 18 to 22 to generate the DFNs representing the sub-horizontal included angles based on the analysis as illustrated in Fig. 3. The sizes of the DFNs were also chosen from 0.1 to 1.0 m. The selection of these parameters allows us to realize the well-cleated coal seam as likely fully persistent discontinuities in the narrow pillar gate-roads system.

Figure 6 presents the rock blocks consisting of cleats and bedding planes in the coal seam explicitly created by the DFN technique. We conducted 10 realizations of the DFN to construct the cleats system in the coal seam. The largely dispersed poles in the stereographic projection, as shown in Fig. 3 indicate the orientation of the DFN in the wide pillar system. The congregated poles in the stereographic projection, as illustrated in Fig. 3 present the orientation of the DFNs in the narrow pillar system. Figure 6(a) shows the blocky coal seam in the wide pillar system where the dip angles of the mean bedding planes are assumed to be 30° from horizontal. Figure 6(b) illustrates the blocky coal seam in the narrow pillar system where the dip angle of the mean bedding plane is horizontal. The cleats in the wide pillar system, as shown in Fig. 6(a) are realized by DFNs with approximately 20% less fracture frequency and cleats half the size of the cleats in the narrow pillar system, as illustrated in Fig. 6(b). These features produce a relatively poorly cleated coal seam by the less persistent cleats in the wide pillar system but produce a relatively well-cleated coal seam by the more persistent cleats in the narrow pillar system. In this way, the included angle between the principal stresses, as illustrated by the arrows in Fig. 6 and cleat orientations govern the anisotropic strength and behavior of the coal.

The contours of the displacements around the gate-roads are presented in Fig. 7. The red contours indicate total displacements greater than 20 cm. This value is equivalent to 10% of the height of the gate road. In the wide pillar system, as shown in Fig. 7 the displacement contours are developed deeper and more localized, whereas the displacement contours in the narrow pillar system show shallow and uniform distributions. This result occurs because of the different degrees of anisotropy represented by the different dips of the DFNs, as explained earlier.

Figure 7(b) and (c) more closely illustrate the deformation around the boundary of the gate-road in the wide pillar system and the narrow pillar system, respectively. The maximum displacement measured on the floor of the gate road in the wide pillar system is about 0.35 m. The maximum displacement measured on the floor of the gate road in the narrow pillar system is about 0.014 m.

Figure 8 presents the contours of maximum shear strain increments associated with the dissipated plastic energy. The maximum contour was cut off at 0.2 m/m, but the maximum shear strain increment in the wide pillar system was much higher than that amount. Therefore, the maximum shear strain increments are developed more extensively in the wide pillar system, Fig. 8(a) than in the narrow pillar system, Fig. 8(b).

The profiles of the vertical displacement across the surface of each floor of the gate roads are shown in Fig. 9. The solid-triangle curve indicates the displacements measured at the gate roads with the wide pillars. The dotted-circle curve presents the displacements obtained at the gate roads with the narrow pillars. The profiles of the vertical displacement across the surface of the floor of the gate roads in the wide pillars become very obvious that the maximum vertical displacement is as large as approximately 1 m with a convex-shaped curve, while the maximum vertical displacement appears as much as about 20 cm with a relatively flat curve at the gate roads with the narrow pillars.

In summary, we have presented the DFN technique for implementing models having different anisotropic characteristics in the floor and coal of the narrow pillar region and the wide pillar region. The results of the numerical modeling matched observations of the relative amounts of heave from each gate-road system.

4 Conclusion

A numerical simulation for understanding the true behavior of a rock mass associated with underground mining was conducted by researchers from the National Institute for Occupational Safety and Health (NIOSH).

3DEC modeling in conjunction with the DFN technique was performed to better understand the true behavior of a floor heave associated with underground mining in the anisotropic stress field. The effect of stress rotation in the mining-induced stress field was considered by using different means of DFN orientation distribution in the coal seam. The wide pillar system had an oblique included angle that was generated by the DFN with higher variability of the orientations. The narrow pillar system had a normally included angle that was generated by the DFN with a lower variability of the orientations.

The spatial characteristics of the discontinuities (i.e., cleats and bedding planes) as input data for the 3DEC model were estimated based on the results of the laboratory tests and the field observation. The DFNs explicitly simulated poorly and well-cleated coal seams, indicating the different spacing between cleat apertures using the probability distribution functions on fracture density (or frequency) and size. The heterogeneity of the engineering properties (i.e., cohesion and tensile strength) were also considered by the Monte Carlo simulations.

The 3DEC models using the DFN technique demonstrated that the results of the modeling agreed with the observations of the relative amounts of heave from each gate-road system. The results represent a more realistic improvement compared to the implicit approach used with the FLAC3D model. The natural fractures as cleats in the coal seam are very significant regarding the coal's anisotropy of strength and brittleness.

We conclude that such characteristics can explain the observed phenomena of floor heave associated with the larger pillars and no significant floor heave associated with the smaller pillar system.

Acknowledgements

Data from this manuscript have been presented at the 40th SME International Conference on Ground Control in Mining, July 27–28, 2021.

References

1. Kim B-H, Larson MK (2019) Numerical investigation of factors involved in a floor heave mechanism in a bump-prone coal mine. Proceedings of the 38th International Conference on Ground Control in Mining. Morgantown, WV, July 23–25, 2019 Society for Mining, Metallurgy, and Exploration, Inc. (SME),, Englewood, CO
2. Itasca Consulting G, Inc., (2019) 3DEC distinct element modeling of jointed and blocky material in 3D. User's guide version 7.0., Itasca Consulting Group, Inc.,. http://docs.itascacg.com/3dec700/3dec/docproject/source/3dechome.html
3. Laubach SE, Marrett RA, Olson JE, Scott AR (1998) Characteristics and origins of coal cleat: a review. Int J Coal Geol 35:175–207
4. Agapito JFT, Goodrich RR (2000) Five stress factors conducive to bumps in Utah, USA, coal mines. Proceedings: 19th International Conference on Ground Control in Mining. Morgantown, WV, August 8–10, 2000 West Virginia University, Morgantown
5. Hebblewhite B, Galvin JM (2016) A review of the geomechanics aspects of a double fatality coal burst at Austar Colliery in NSW, Australia in April 2014. Proceedings: 35th International Conference on Ground Control in Mining. Morgantown, WV, July 26–28, 2016 West Virginia University, Morgantown
6. Kim BH, Larson MK (2017) Evaluation of bumps-prone potential regarding the spatial characteristics of cleat in coal pillars under highly stressed ground conditions. Proceedings, 51st U.S. Rock Mechanics/Geomechanics Symposium. San Francisco. June 25–28, 2017 American Rock Mechanics Association (ARMA), Alexandria, VA, 8
7. Kim B-H, Walton G, Larson MK, Berry S (2018) Experimental study on the confinement-dependent characteristics of a Utah coal considering the anisotropy by cleats. Int J Rock Mech Min Sci 105:182–191
8. Robeck ED (2005) The effects of fault-induced stress anisotropy on fracturing, folding and sill emplacement: insights from the Bowie Coal Mines, Southern Piceance Basin, western Colorado. M.S. thesis, Brigham Young University

9. Lawson HE (2015) Verbal conversation between Heather Lawson and Larson MK, July 29.
10. Tesarik DR, Whyatt JK, Larson MK (2013) Inferring mine floor properties from pillar size and floor heave. Proceedings of the 47th U.S. Rock Mechanics/Geomechanics Symposium. San Francisco, CA, June 23–26, 2013 American Rock Mechanics Association, Alexandria, VA
11. Farmer IW (1968) Engineering properties of rocks. E. & F. N. Spon, London
12. British Geological Survey (2002) Engineering geology of British rocks and soils, mudstones of the Mercia Mudstone Group, Urban Geoscience and Geological Hazards Programme. Research Report RR/01/02
13. Clark IH (2006) Simulation of rockmass strength using ubiquitous joints. Proceedings of the 4th International FLAC Symposium on Numerical Modeling in Geomechanics. Madrid, Spain, May 29–31, 2006 Itasca Consulting Group, Inc., Minneapolis, MN
14. Pierce M, Cundall P, Ivars DM, Darcel C, Young RP, Reyes-Montes J (2006) Six monthly technical report, caving mechanics, sub-project no. 4.2: research and metholodogy improvemenet, and sub-project 4.3: case study application. Report to Mass Mining Technology Project, Itasca Consulting Group, Minneapolis, MN
15. Sainsbury B, Pierce M, Mas Ivars D (2008) Simulation of rock mass strength anisotropy and scale effects using a ubiquitous joint rock mass (UJRM) model. Continuum and Distinct Element Numerical Modeling in Geo-Engineering — 2008, Proceedings of the 1st International FLAC/DEM Symposium. Minneapolis, MN, August 25–27, 2008 Itasca Consulting Group, Inc., Minneapolis, MN
16. Board M, Pierce ME (2009) A review of recent experience in modeling of caving. Proceedings of the International Workshop on Numerical Modeling for Underground Mine Excavation Design. Asheville, NC, June 28, 2009 U.S. Department of Health and Human Services, National Institute for Occupational Safety and Health (NIOSH), Pittsburgh, PA

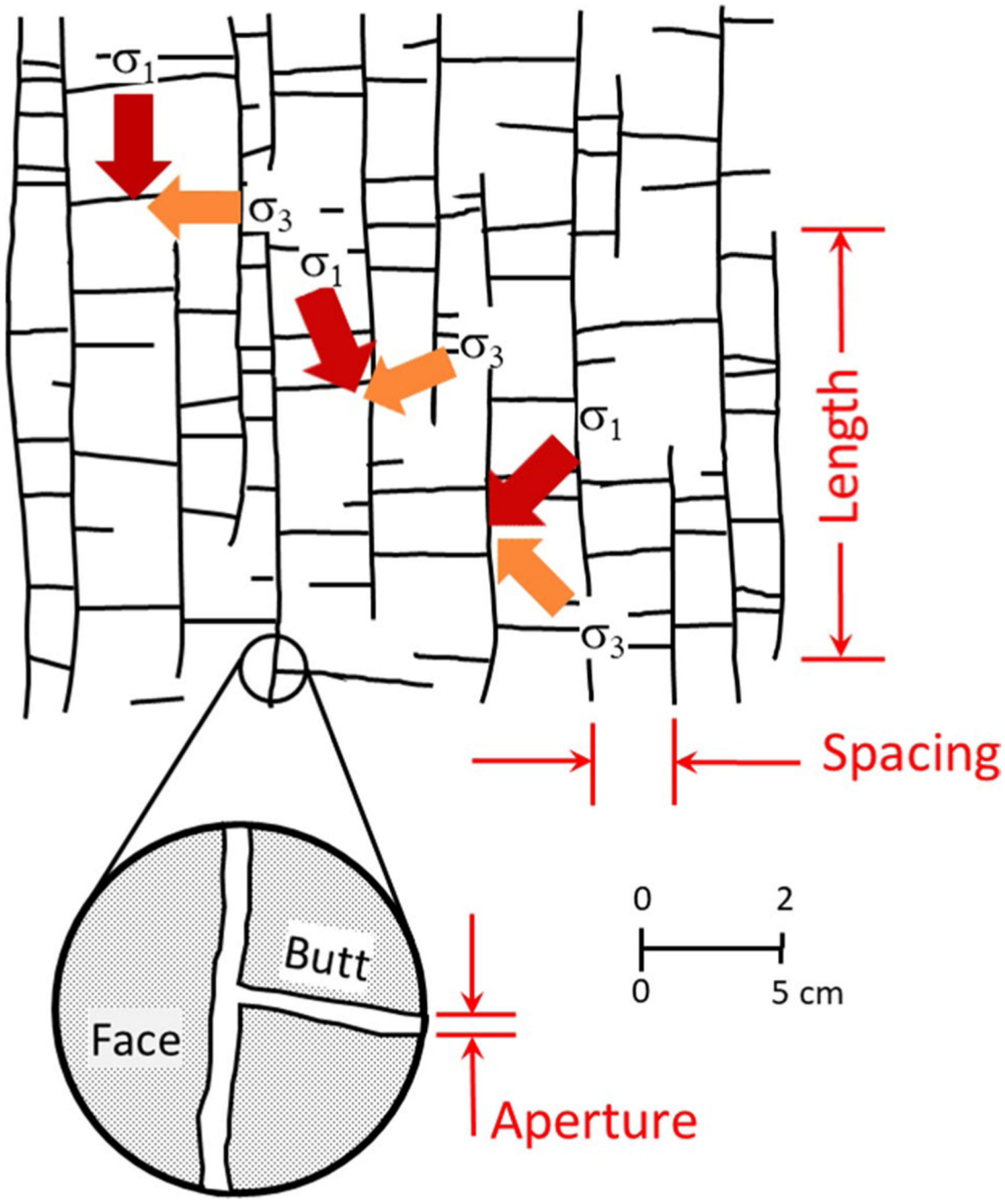

Fig. 1.
Cleat hierarchies in cross-section view (after [3])

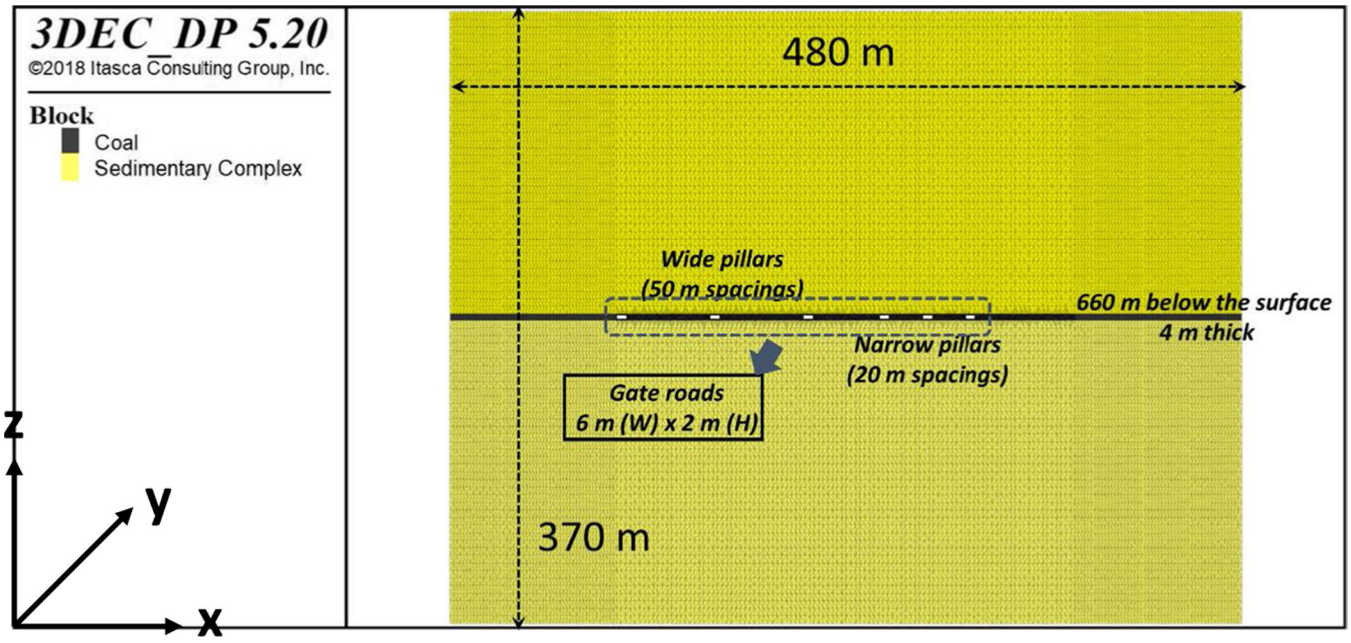

Fig. 2.
Layout of the 3DEC model (not to scale)

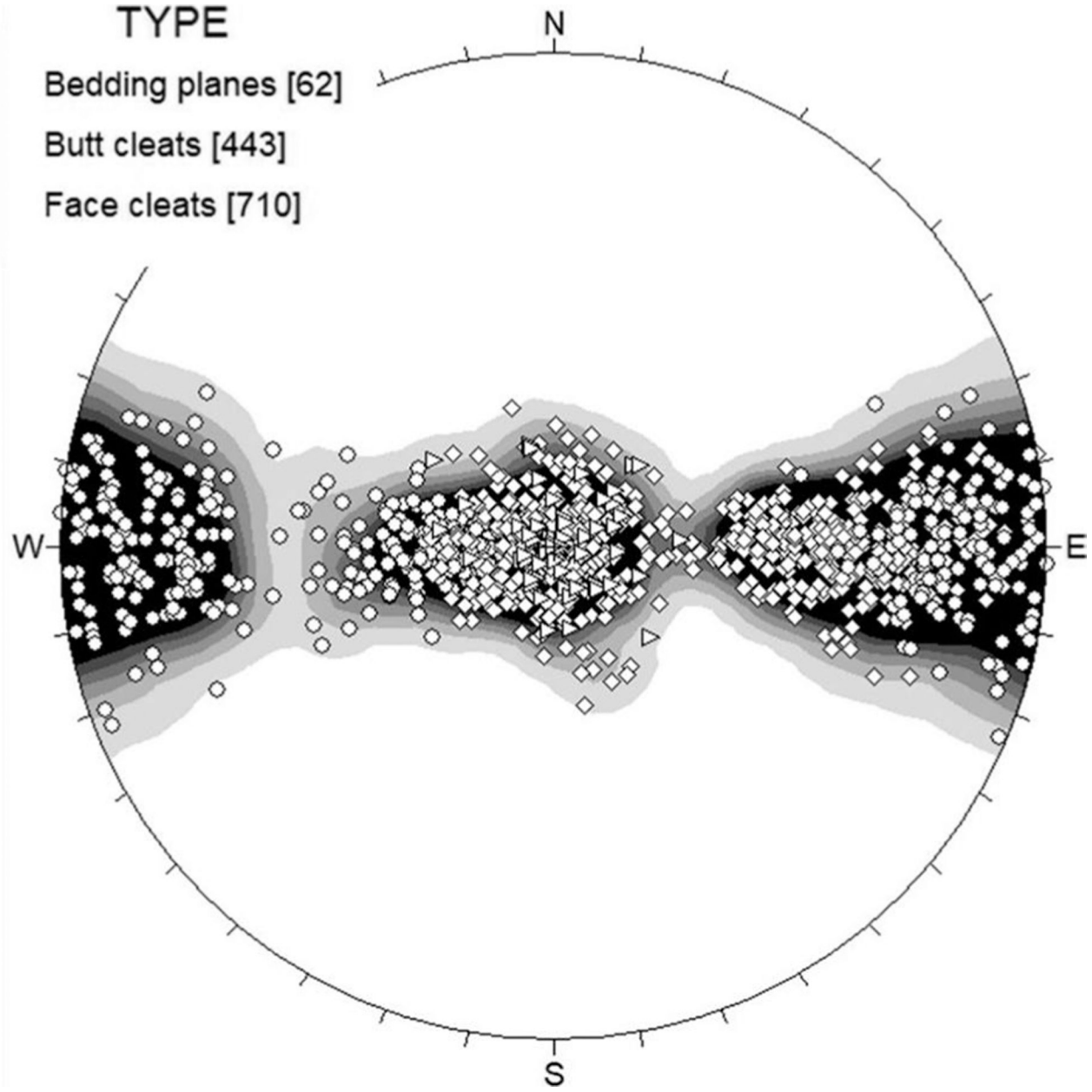

Fig. 3.
The orientations of the cleats and bedding planes are plotted in a stereographic projection

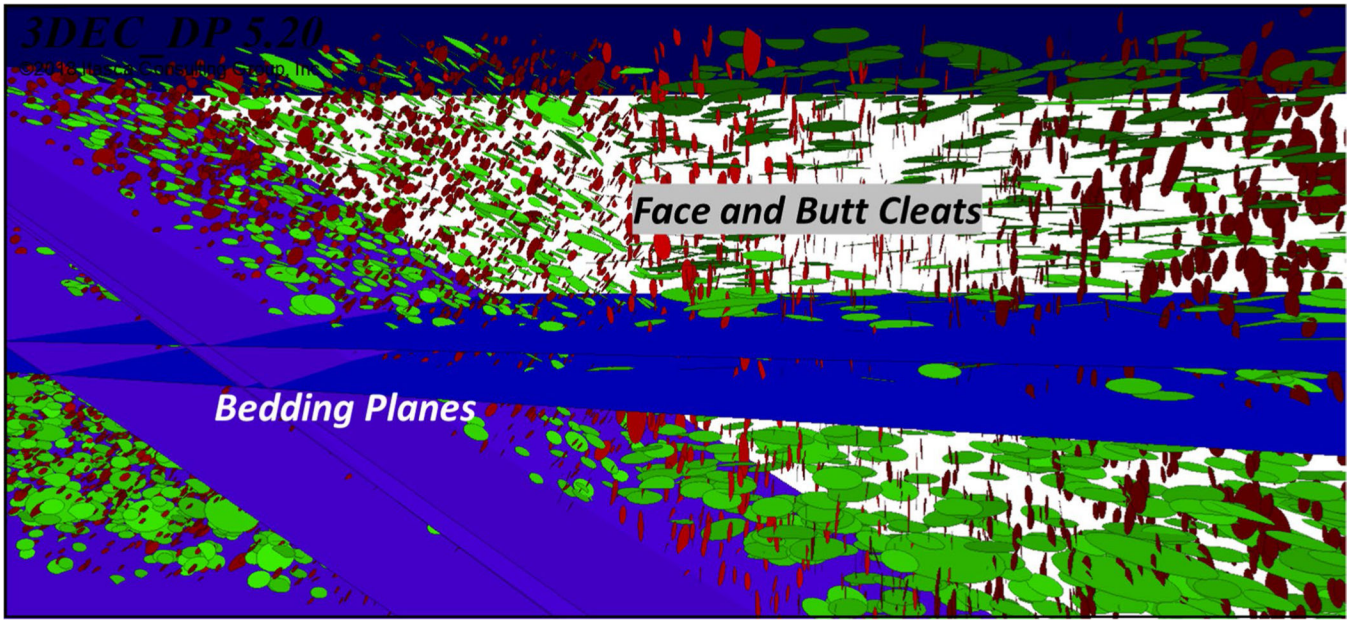

Fig. 4.
Face and butt cleats (red and green disks) perpendicular to bedding planes (blue planes) created by the DFNs

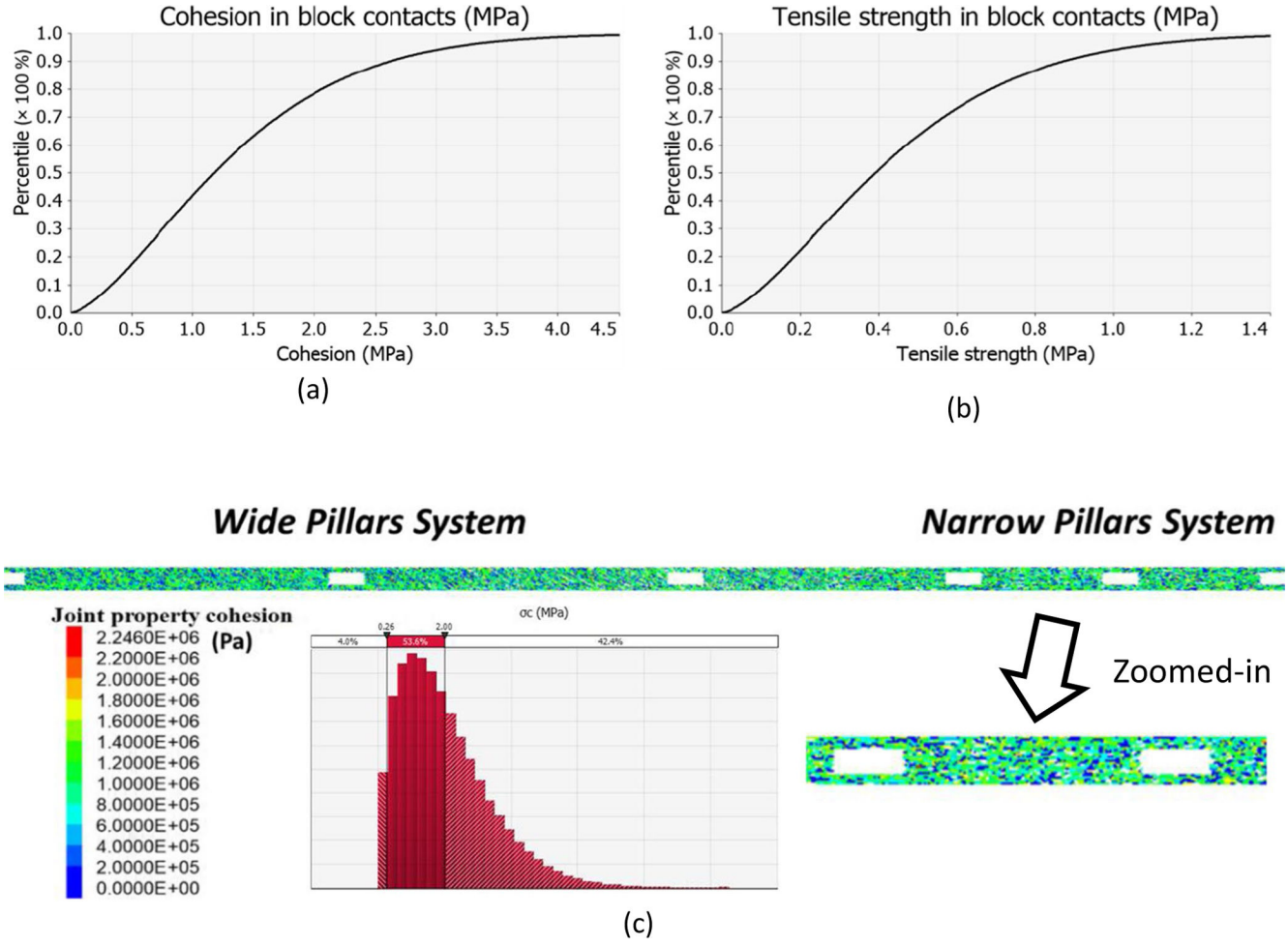

Fig. 5.

The probability distributions generated by the Monte Carlo simulation [**a** cohesion and **b** tensile strength] and **c** the assigned cohesion (histogram: distribution of the cohesion) for (sub-) contacts of blocks in the 3DEC model

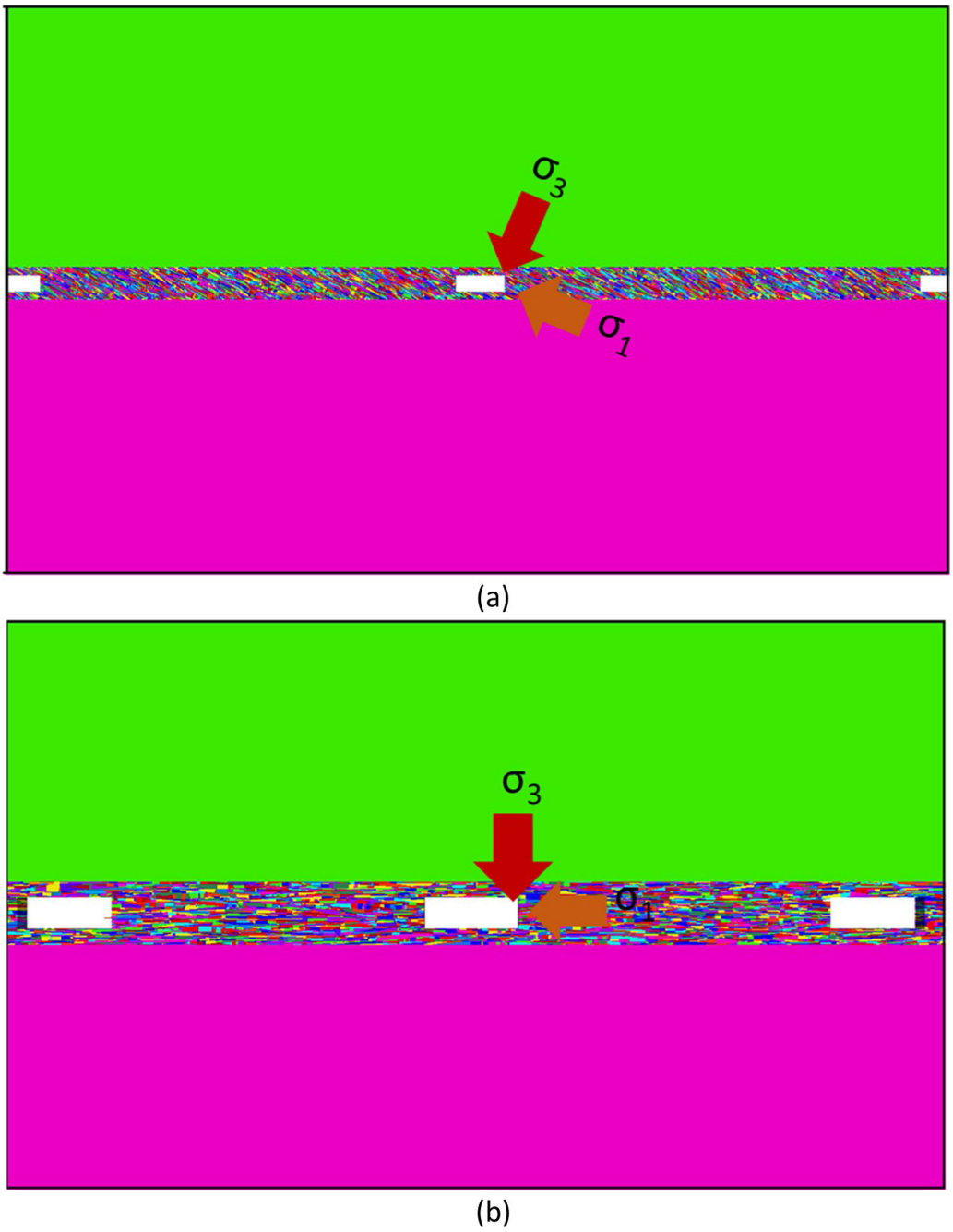

Fig. 6.

Introduced discrete fracture networks for cleats and bedding planes in the vicinity of gate roads in **a** wide pillar and in **b** narrow pillar

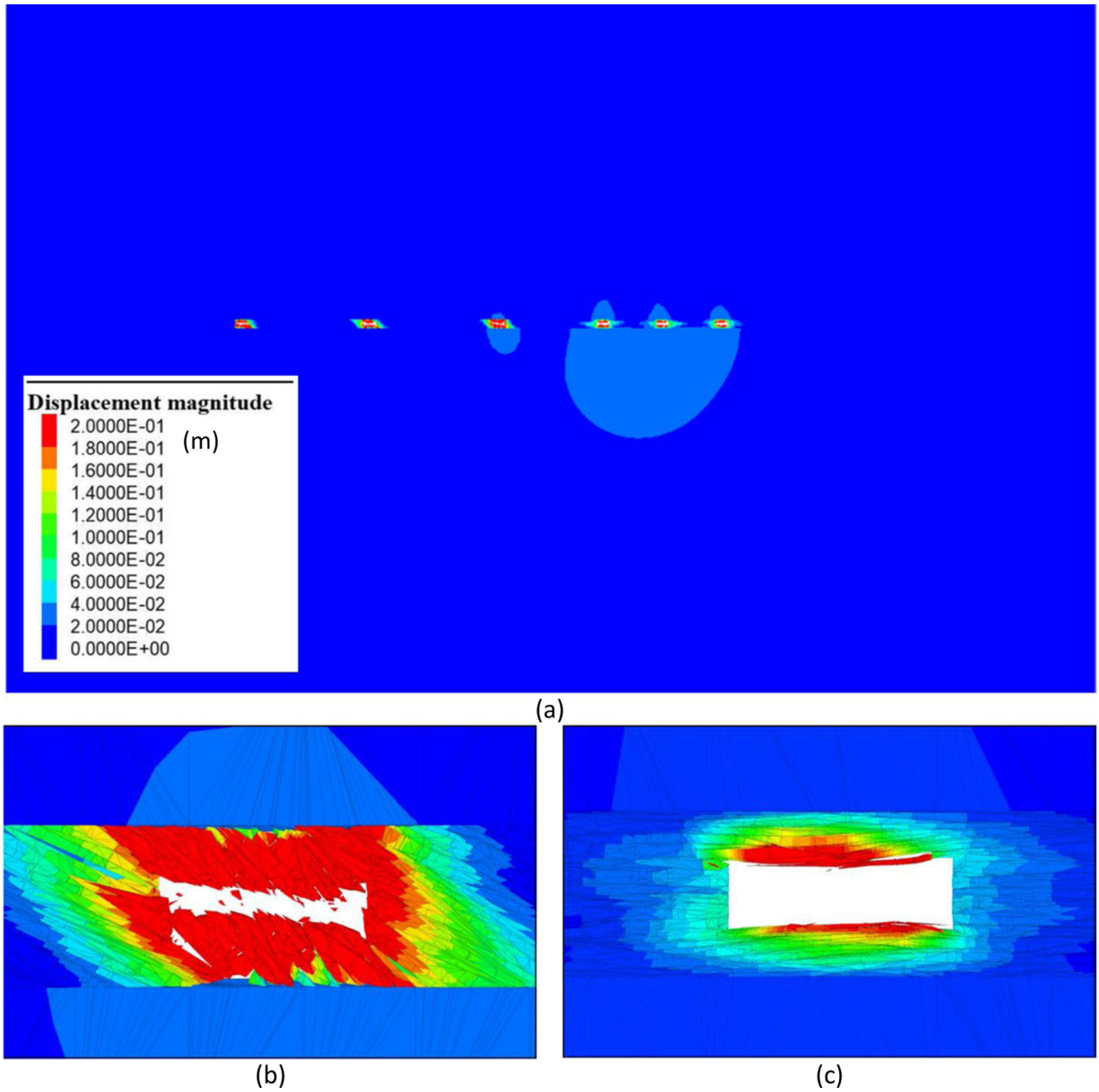

Fig. 7.

a The contours of displacement calculated in the 3DEC model, **b** the contours of displacement and profile of deformation of the gate road in the wide pillar system, and **c** the contours of displacement and profile of deformation of the gate road in the narrow pillar system

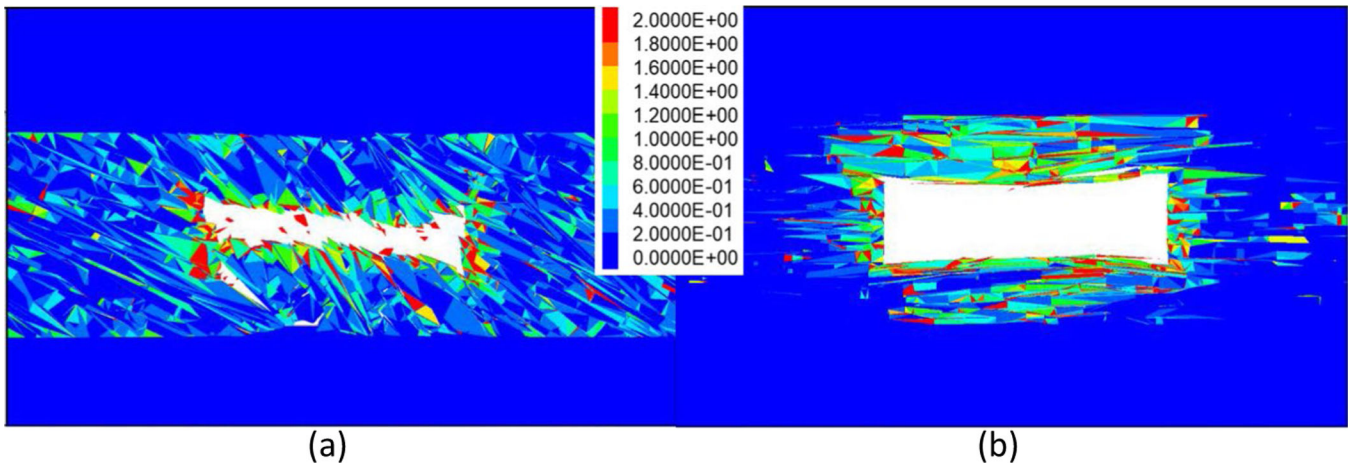

Fig. 8.

a The contours of maximum shear strain increments around the gate road in the wide pillar system, and **b** the contours of maximum shear strain increments around the gate road in the narrow pillar system

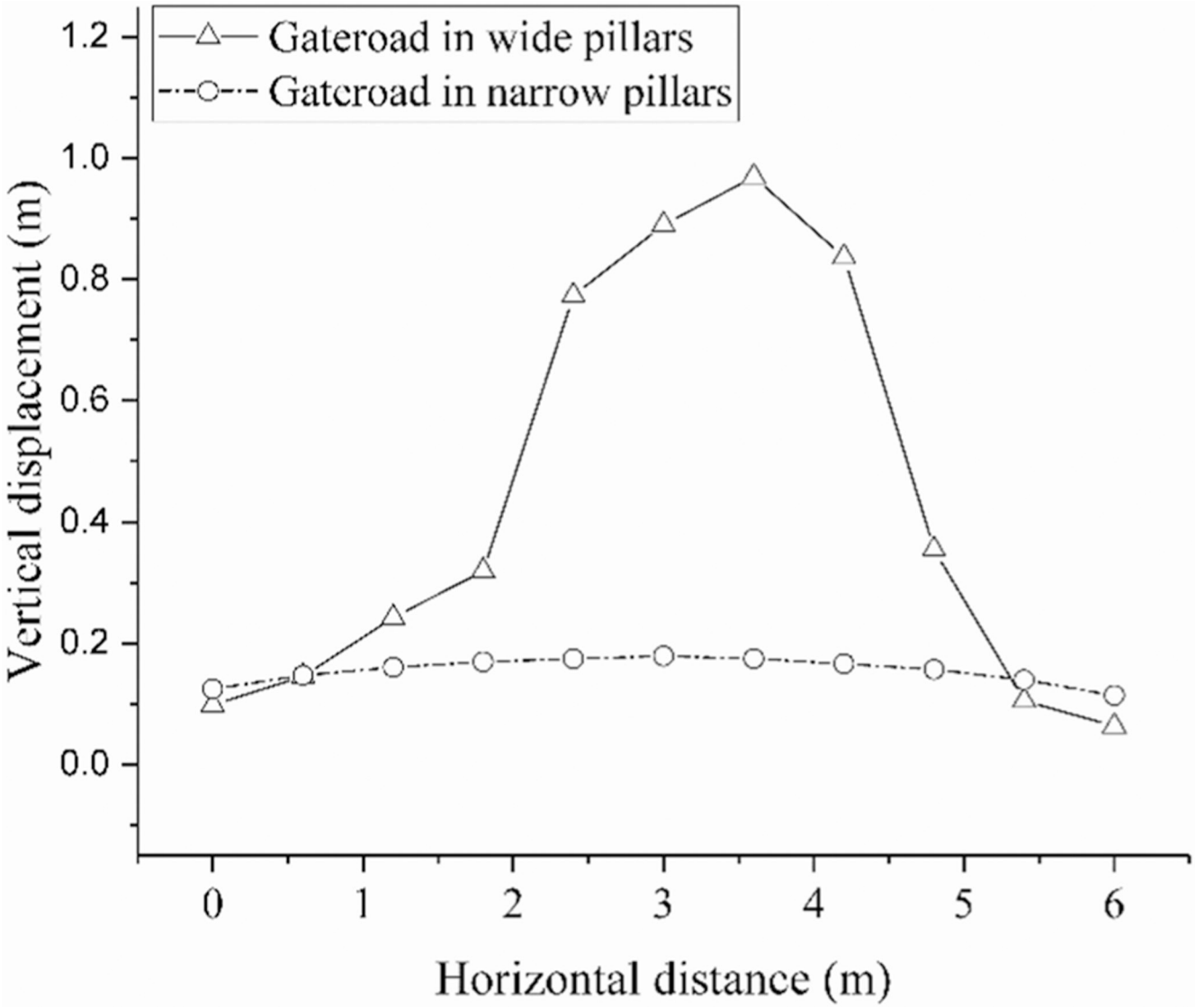

Fig. 9.
Profiles of vertical displacement across the gate road floor measured in the 3DEC model

Table 1

Input data for the seam and the surrounding rocks in the 3DEC model

Zone group	Young's modulus (GPa)	Poisson's ratio	Joint properties				
			Normal stiffness (GPa/m/m)	Shear stiffness (GPa/m/m)	Cohesion (MPa)	Friction angle (°)	Tensile strength (MPa)
Seam	3.8	0.25	105	52.5	1.35 (±0.91)	35	0.45 (±0.30)
Top	20.7	0.2	-	-	-	-	-
Bottom	9.8	0.25	-	-	-	-	-